

Geometry of Fully Wiped Twin-Screw Equipment

M. L. BOOY

*Engineering Technology Laboratory
E. I. du Pont de Nemours & Company (Inc.)
Wilmington, Delaware 19898*

The cross section geometry of fully wiped corotating twin screws is derived from simple kinematic principles. A pair of screws can have identical cross sections with each screw running at the same speed, or they can have an unequal number of tips and rotate at different speeds. The more conventional case of equal cross section is reviewed in detail, showing how screw diameter, centerline distance, lead, and number of tips influences design, net volumes, and surface areas. The screw cross section is unique for a given diameter, centerline distance, and number of tips. The construction of the cross section is shown, both for pairs of identical screws, and for screws with a speed ratio. Maps are provided to show applicability of screws with 1, 2, and 3 tips.

INTRODUCTION

For the past 20 years twin-screw equipment has been used in polymer processing for extrusion, pumping, mass and heat transfer, and polymerization. In the intermeshing type of twin-screw equipment, which is the concern of this paper, one screw wipes its mate, and vice versa. It is this wiping action that makes twin-screw equipment attractive for handling many polymers, since it eliminates dead spots where polymer can collect, stagnate, and return degraded to the mainstream.

The most common twin-screw equipment comprises a housing, or barrel, and two parallel shafts equipped with identical- or opposite-hand screw or paddle elements. The identical screws rotate in the same direction at the same speed (1); the opposite-hand screws rotate at the same speed, but in opposite direction. A thorough knowledge of the geometry of twin screws is essential for designing the equipment and for analyzing fluid transport and heat and mass transfer therein. The free volume between screws and barrel must be known, as well as screw and barrel surface areas.

The cross section of a twin screw has a unique shape for a given diameter, centerline distance, and number of parallel channels because of the requirement that one screw must, in any position, wipe its mate. This unique shape is determined by means of a well-known kinematic principle. Kinematic analysis yields equations that relate the major design parameters and, in graphical form, serve as the basis for design and selection of screw dimensions. Volumes and surface areas can be calculated, once the major parameters have been selected.

Our analysis mainly concerns twin screws corotating at the same speed. It is shown how a reasonable flow analysis can be made by substituting a single screw as a model. The remaining analysis deals with the less conventional cases of twin screws corotating at different speeds and those having different diameters.

KINEMATICS AND CROSS SECTIONS OF SCREWS COROTATING AT THE SAME SPEED

The simplest pair of corotating screws are a set of identical screws with the same diameter, the same lead, and the same speed and direction of rotation. In this analysis we ignore clearances and assume that one screw wipes its mate with an infinitesimal or zero clearance. Figure 1 shows typical cross sections through pairs of corotating twin screws, all with different numbers of tips, n . For ease of comparison all screws are shown with the same radius R_s , but, as shown in Fig. 1, the centerline distance C_L is not the same for all cases.

We can think of a screw with a given cross section as being obtained by uniformly twisting a bar with that

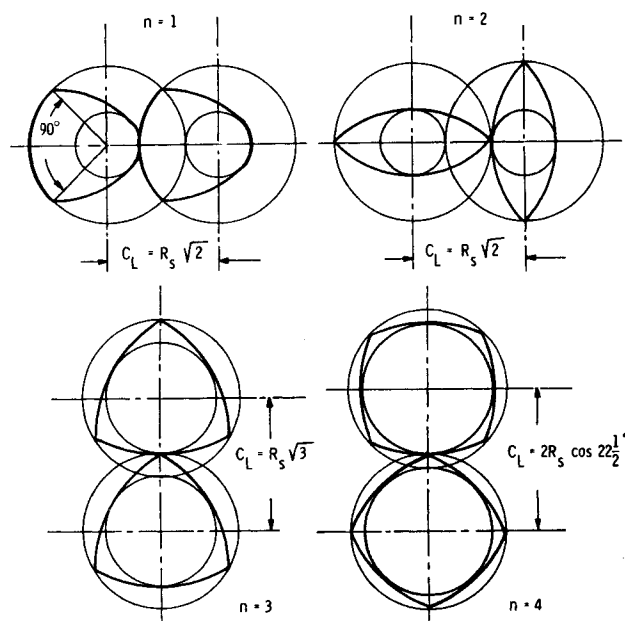


Fig. 1. Typical cross sections through pairs of screws with 1, 2, 3, and 4 tips.

cross section. Thus, the screw is also an infinite set of infinitely thin discs, each rotated slightly with respect to its neighbor. Since all pairs of discs are fully wiped when the screws are fully wiped, we have only to study one pair to determine screw cross section.

The construction of that cross section will be shown for a pair of discs with one tip for given centerline distance C_L , and screw radius R_s . In Fig. 2, let P_0Q_0 be the tip of disc B. We want to know the shape of disc A that is mathematically wiped by tip P_0Q_0 , which means that we must construct the path of P_0Q_0 relative to disc A. Construction of that path becomes simple when we add a motion to the system of discs A and B which brings disc A to a standstill. Initially both discs rotate clockwise at a speed N . Disc A is brought to a standstill when we add a counterclockwise rotation ($-N$) around 'O'. Now center 'C' of disc B rotates counterclockwise around 'O' with a rotational velocity $-N$, describing a circle with radius C_L and center at 'O'. At the same time, disc B stops rotating around its center.

Disc B does not rotate in the relative motion, so all points of that disc describe circles with radii equal to C_L . In the position shown, the relative velocity of C_0 is perpendicular to the x-axis. The velocity of P , or of any point of disc B, is at that instant perpendicular to the x-axis, so the trajectory of P must have its center M_p on the circle through the tips of disc A. Similarly, M_q is the center of the circular trajectory of Q . Figure 2 shows the trajectories of both P and Q .

Figure 3 shows different positions of tip PQ during the relative motion. C_1 and C_2 are so selected that the lines C_1Q_1 and C_2P_1 pass through 'O'. Between C_1 and C_2 the contour of disc A is wiped by the circular tip PQ ; outside this zone the contour consists of the trajectories of P and Q . The envelope of all positions of the circular tip PQ is a circular arc Q_1P_1 with radius equal to $R_B = C_L - R_s$ obtained when C moves between C_1 and C_2 . The angle Q_1OP_1 is equal to the tip angle α . Thus, the contour is bounded by the circular arc Q_1P_1 with radius R_B , the trajectories of P and Q with radius C_L , and the tip circle with radius R_s .

The wiping velocity between the tip of one disc and the flank of its mate is used in shear rate and energy calculations. All points of disc B have relative velocities

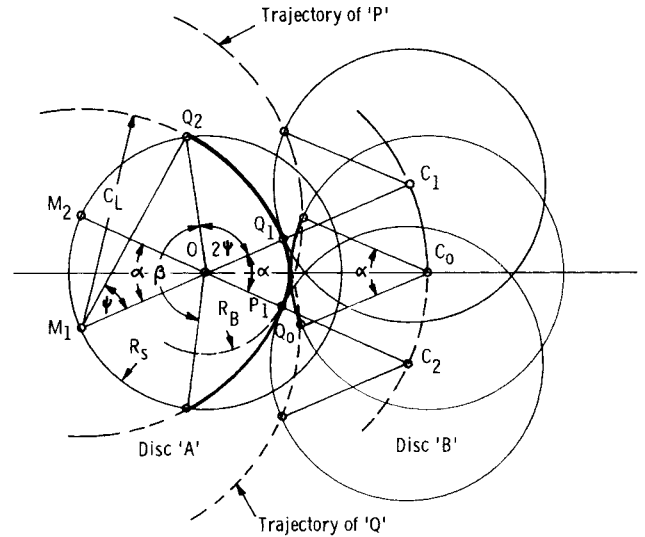


Fig. 3. Envelope of positions occupied by tip arc P,Q , during relative motion.

that in all positions are equal to the relative velocity of the center C of disc B. Thus, the wiping velocity is equal to U_{C_0} , which is $2\pi N C_L$.

In the construction of Fig. 3 we did not impose the requirement that both screws must have the same tip angles. For discs with a single tip Fig. 3 shows a tip angle β for disc A much larger than tip angle α of disc B. The root angle Q_1OP_1 of disc A is the same as the tip angle α of disc B. Inversely, the root angle of disc A is the same as the tip angle of disc B. We restrict this analysis to cross sections with the same tip and root angles for both discs and will derive the conditions for which this is the case. Introduce angle ψ , which is:

$$\psi = \cos^{-1}(C_L/2R_s) = \cos^{-1}(\rho_c/2) \quad (1)$$

The dimensionless parameter ρ_c is the ratio of the centerline distance to the barrel radius, called the centerline ratio for short. Now $\angle Q_1OQ_2 = 2\psi$, so summing angles around 'O' we find:

$$\alpha + \beta + 4\psi = 2\pi \quad (2)$$

For symmetrical cross sections ($\alpha = \beta$) with one tip, the tip angle is equal to:

$$\alpha = \pi - 2 \cos^{-1}(\rho_c/2) \quad (3)$$

The construction of fully wiped discs with more than one tip ($n > 1$) is quite similar but now Eq 2 must be modified for symmetrical cross sections to include the number of tips n . Then:

$$n(2\alpha + 4\psi) = 2\pi \quad (4)$$

Substitution of Eq 1 in Eq 4 yields the relation between tip angle α and centerline distance ratio ρ_c :

$$\rho_c = 2 \cos(\pi/2n - \alpha/2) \quad (5)$$

That ratio is shown in Fig. 4 as a function of tip angle α with n as parameter. This figure shows some of the major factors governing twin-screw equipment design. The

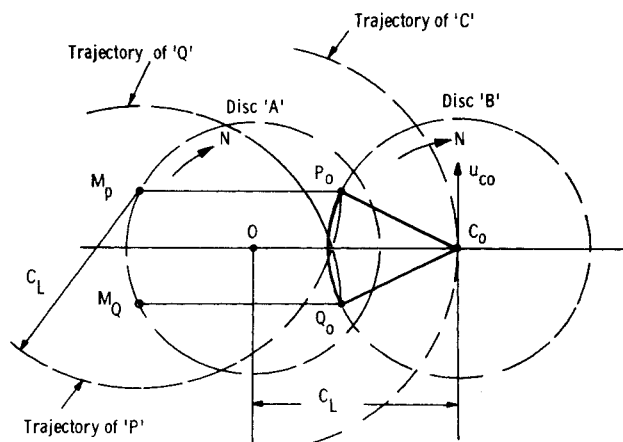


Fig. 2. Construction of trajectories for P and Q .

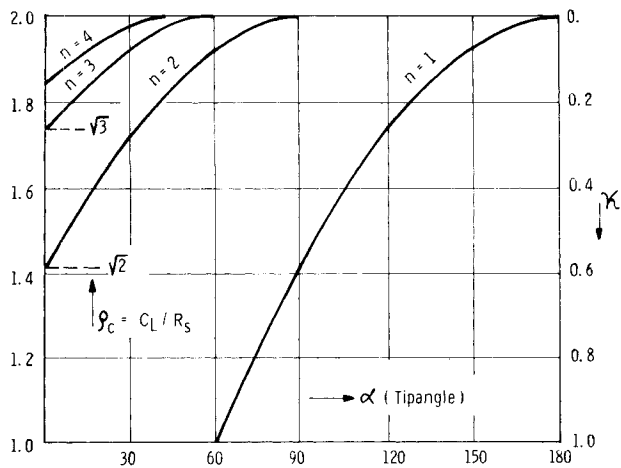


Fig. 4. Centerline ratio ρ_c as function of tip angle α with number of tips as parameter for pairs of identical screws.

ratio ρ_c is immediately fixed by the housing design, which is frozen when C_L and R_s are specified. The curves then show which types of screw can be accommodated. For instance, α becomes zero for $\rho_c = \sqrt{2}$ when screws with two tips are used. The tip angle becomes 90° for screws with one tip and the same value of ρ_c , while screws with three tips cannot be accommodated since α would be negative. Similarly, α is zero at $\rho_c = \sqrt{3}$ for $n = 3$, at $\rho_c = 2 \cos 22\frac{1}{2}^\circ = 1.848$ for $n = 4$. The channel depth of a screw is given by:

$$h = 2R_s - C_L \quad (6)$$

The relative channel depth κ is defined here as:

$$\kappa = h/R_s = 2 - \rho_c \quad (7)$$

This parameter is shown on the scale at the right side of Fig. 4. For $n = 1$ the ratio ρ_c becomes 1.0 when $\alpha = 60^\circ$. At that ratio the relative channel depth κ is 1.0, or the channel depth is equal to the radius R_s , as also shown in Fig. 5. Such a design would be impractical in most cases since there is no shaft remaining at the drive end to drive the screw.

The relative motion of one disc with respect to its mate is illustrated in Figs. 6-7. In each case disc 'B' is

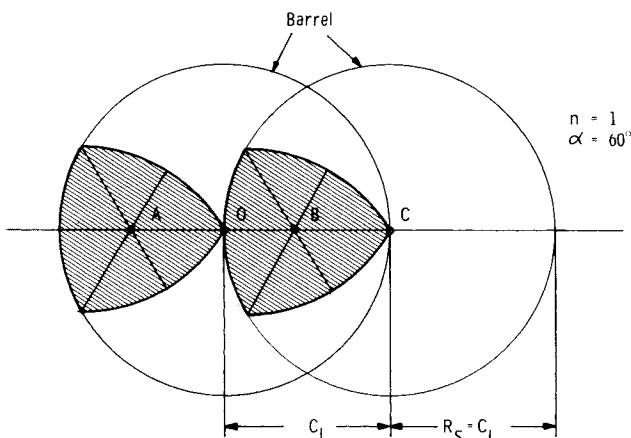


Fig. 5. Limiting case for screws with one tip and channel depth equal to screw radius.

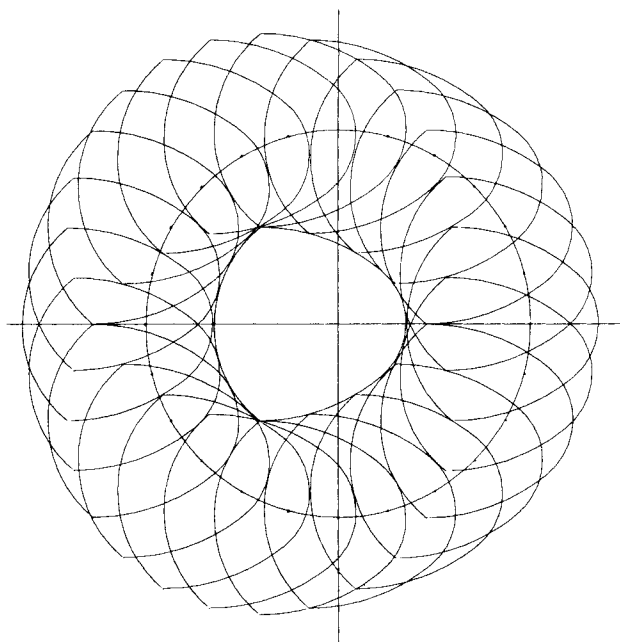


Fig. 6. Relative motion for discs with one tip, $\rho_c = 1.55$.

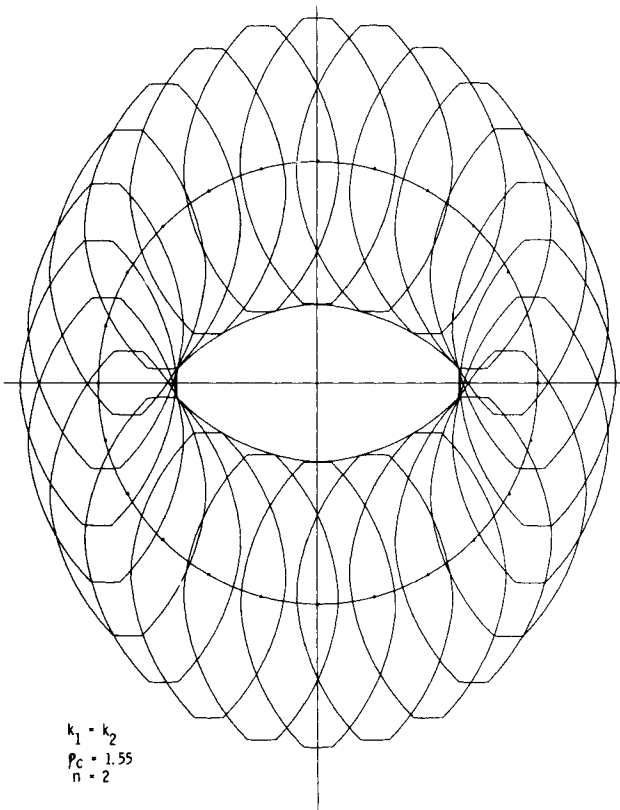


Fig. 7. Relative motion for discs with two tips, $\rho_c = 1.55$.

shown in 24 positions with disc 'A' at a standstill. It should be noted that disc 'A' is the inner envelope of all possible positions of disc 'B'.

In the previous figures we showed screw cross sections for which the centers of rotation were located within those cross sections. A limiting case is shown in Fig. 5 where the centers of rotation lie on the periphery.

In some devices the centers of rotation lie outside the cross sections, as shown in Fig. 8, where disc A rotates around O, disc B around C (2, 3). The relative motion of disc B is again obtained adding an opposite rotation around O to the whole system. Now C follows a circular trajectory around O with radius equal to C_L . Disc B loses its rotation and PC remains horizontal; so the trajectory of P is again a circle with radius C_L obtained by moving the trajectory of C horizontally over a distance equal to the eccentricity. Figure 8 shows the resulting trajectories of the tips P, Q, and R. It also shows by the dotted lines a different actual position of the cross sections.

Before discussing other properties of these screws we will first discuss the more general case of screws with a diameter and/or a speed difference.

CROSS SECTIONS OF SCREWS WITH DIAMETER AND/OR SPEED DIFFERENCES

The screws discussed above are a special case of the more general group of corotating fully wiped screws with a diameter difference or a speed difference. Again we restrict the discussion to pairs of fully wiped discs. The construction of the contours, which is similar to but more complex than the previous construction, is shown in Appendix A.

Now the system has a speed ratio m and two centerline distance ratios, one for each diameter. Equations are given for the shape of the flank curves (Eq A-6) which are no longer circular. It was found more convenient to use the inverse centerline ratios k_1 and k_2 (Eq A-1). The tip angle α can be expressed in k_1 , k_2 , in the speed ratio m , and in the number of tips of one disc. In Eq A-17 we assume that a disc or cross section has the same tip angle α and root angle β . These angles must be positive, which leads to Eq A-10 for the minimum usable speed ratio m . Figure 9 shows the equation for $n_1 = 1$, or for disc A with one tip.

For the simpler case of equal diameters ($k_1 = k_2$) one can derive a relation among ρ_c , m , n , and α (Eq A-22), which results in curves (Fig. 10) similar to Fig. 4.

At present only one vendor uses a speed ratio different from 1.0, but different ratios of speed and diameter have been proposed (2). Figure 11 shows the relative

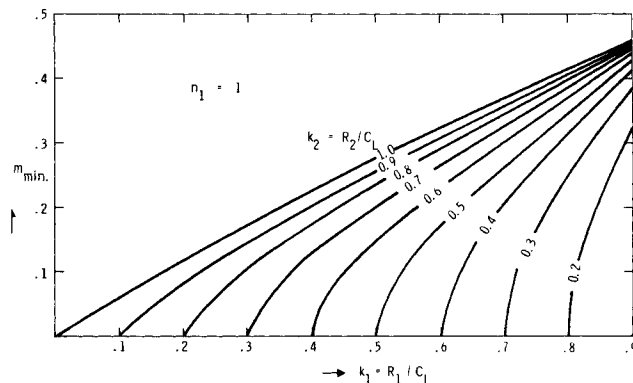


Fig. 9. Minimum usable speed ratio for pair of screws, one of which has one tip.

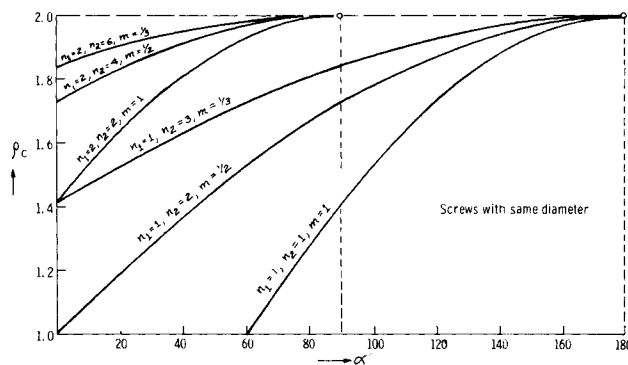


Fig. 10. Centerline ratio ρ_c as function of tip angle α for pairs of screws with speed ratio not limited to $m = 1$.

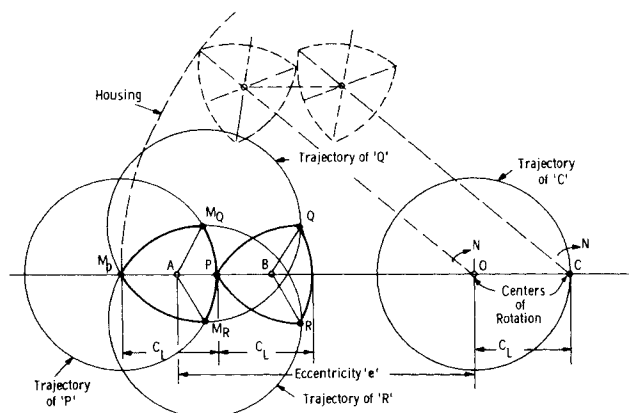


Fig. 8. Relative and absolute motion for the case in which the centers of rotation lie outside the disc cross sections.

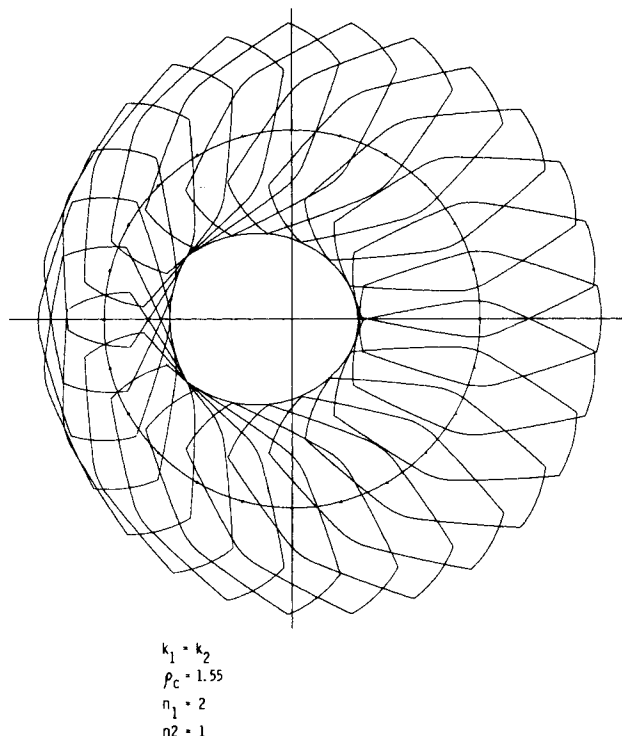


Fig. 11. Relative motion of a pair of screw cross sections with the same diameter and a speed ratio $m = 2$.

motion of cross sections for screws with the same diameter and a speed ratio of 2.0. *Figures 12-14* show relative motions of cross sections with a diameter difference and speed ratios of 2, 3, and 4 respectively. There have been few applications of the more general geometry, and so we will concentrate on conventional screws with equal diameter and equal speed.

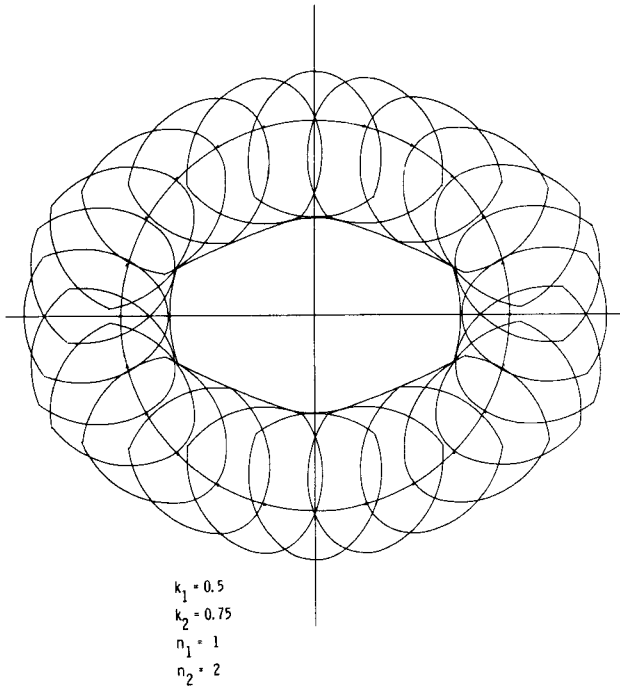


Fig. 12. Relative motion of a pair of screw cross sections with unequal diameters and a speed ratio $m = 0.5$.

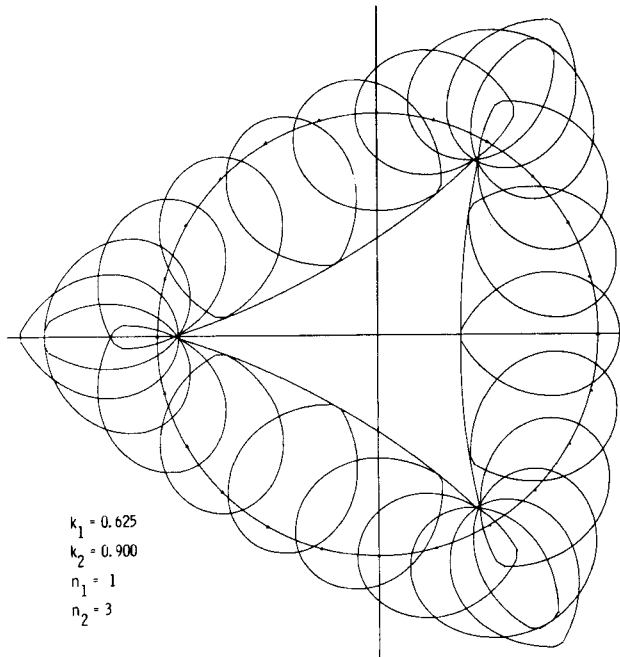


Fig. 13. Relative motion of a pair of screw cross sections with unequal diameters and a speed ratio $m = 0.333$.

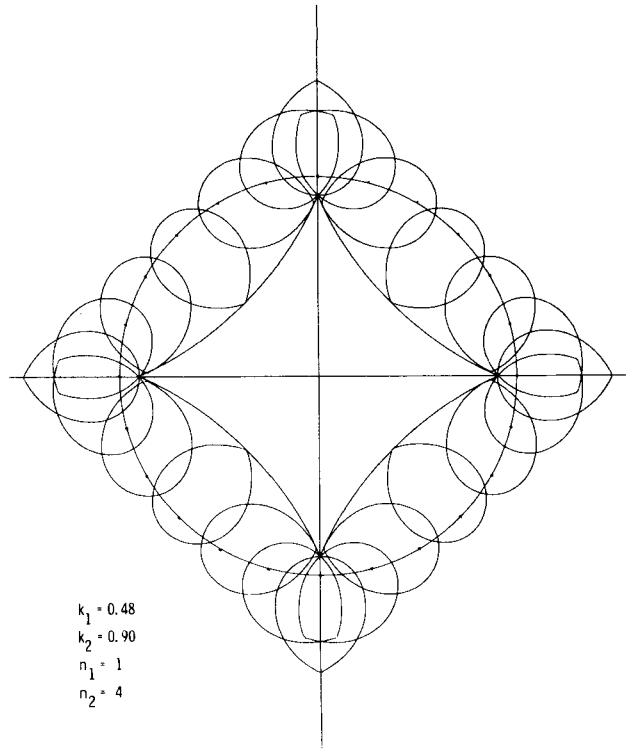


Fig. 14. Relative motion of a pair of screw cross sections with unequal diameters and a speed ratio $m = 0.25$.

GEOMETRIC PROPERTIES

Conventional corotating screws have cross sections similar to those of *Fig. 1*, but they are generally designed to have a non-zero tip angle. *Figure 4* shows how ρ_c must be selected to provide a specified tip angle. For instance, a screw with 2 tips has a tip angle of 20° when the centerline ratio is 1.638, according to *Eq 5*. In general we know the centerline distance and the screw diameter and want to construct the cross section for a given number of tips. That construction is shown in *Fig. 15* for a cross section with 2 tips and $\rho_c = 1.60$. First *B* is located such that $AB = C_L$, which defines ψ and $\Delta COB = 2\psi$. Next point *D* is located such that $\Delta DOC = \pi/n$. Now point *P* is located on the circle midway between *B* and *D*. Make $PD = DQ$, then one tip is bounded by *P*

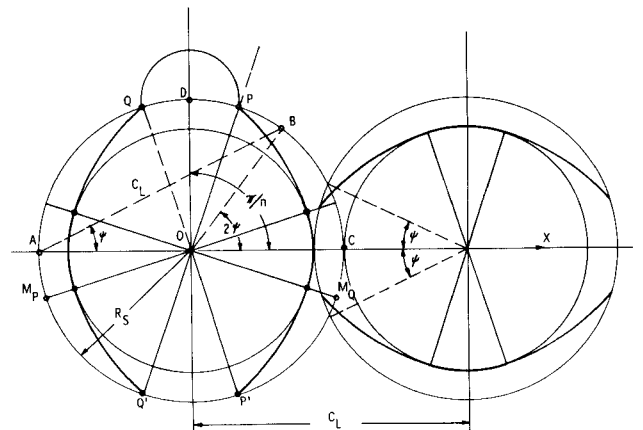


Fig. 15. Basic construction of identical screw cross sections.

and Q . The second tip $P'Q'$ is located symmetrically with respect to the x -axis. Typically the center M_p of the flank curve through P lies on the OD circle at a distance C_L from P , while the root curve is part of the circle that touches the OD circle of the mating screw. The root curves are generally bounded by points on the lines through O and the centers of the flank curves.

Figure 16 schematically shows cross sections in planes perpendicular to and through the axis. Points P_1 and P_2 on the centerlines through two adjacent tips are at an axial distance t/n , or at an angular distance $2\pi/n$. The channel depth is constant between B_1 and B_2 , a function of θ between B_1 and A_1 . At C we introduced the origin for the axial coordinate z , which is related to θ by:

$$z = t\theta/2\pi \quad (8)$$

The channel depth h_θ becomes

$$h_\theta = R_s(1 + \cos \theta) - \sqrt{C_L^2 - R_s^2 \sin^2 \theta} \quad (9)$$

Figures 1 and 15 show that there is a seal in the nip where the wiping occurs, preventing liquid from passing through that nip. This is also schematically shown in Fig. 17, where we show approximate cross sections through the two screws. For instance, in Fig. 17b a plane through the axis O and point F_2 and one through axis C and point F_2 are simultaneously developed into one plane to show the approximate mesh of the screws. The cross section of one pocket between the screws is hatched, demonstrating that the screws form a seal.

In many applications corotating equipment is used to pump very viscous liquids. It is important to realize that twin-screw pumps are not positive-displacement pumps, since channels are continuous and in open communication with inlet and discharge. This is shown schematically in Fig. 18.

Figure 18a shows two cross sections of screws with 3 tips in the position where two tip points coincide at point S . Figure 18b shows the 8-shaped barrel unwrapped into a plane, together with the 'footprints' of the tips. It also shows the axial lines through saddle points S and T . In the figure we unwrapped the barrel a few times to demonstrate the continuity of screw channels. Points A , S , and B of Fig. 18a correspond to the same points in Fig.

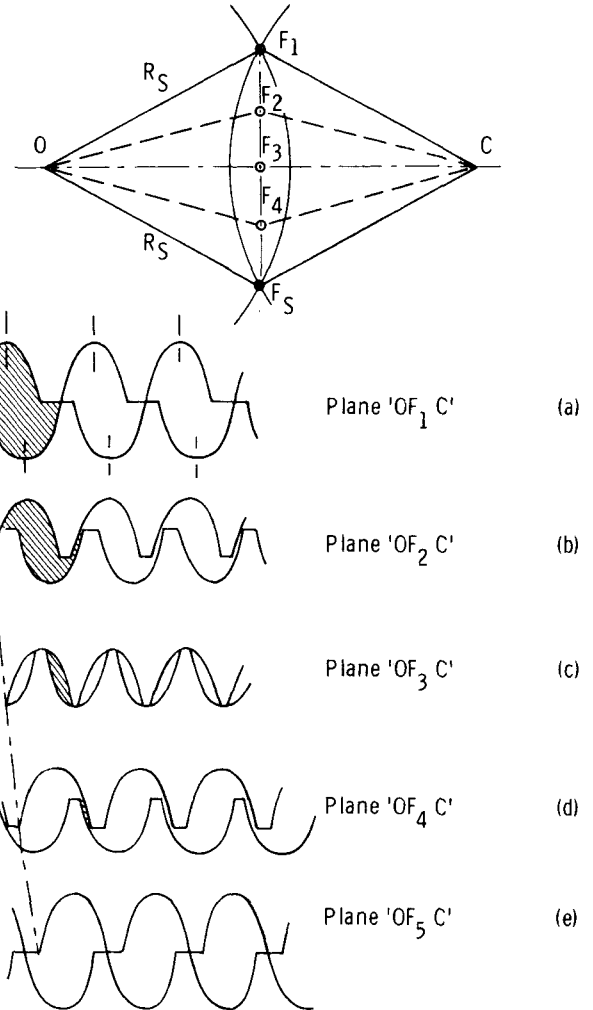


Fig. 17. Screw engagement in the nip zone.

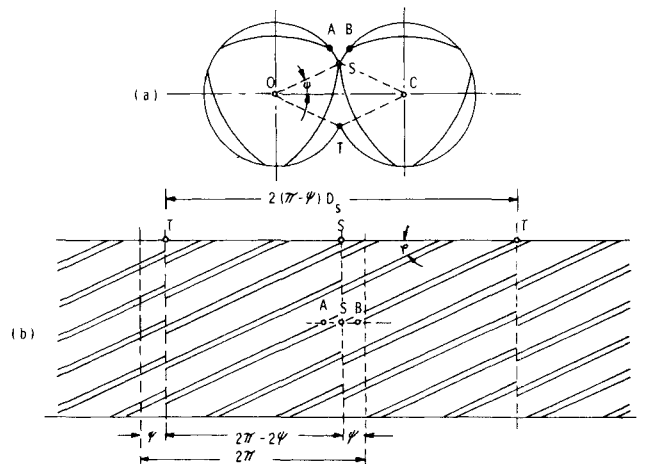


Fig. 18. Development of eight-shaped barrel with footprint of the screw tips.

18b. The tips become slanted lines, which make angles with the tangential direction equal to the helix angle. The tips slide over each other at S . The tip width is generally small with respect to the axial pitch, so in most cases there is an almost continuous channel from one screw to the other.

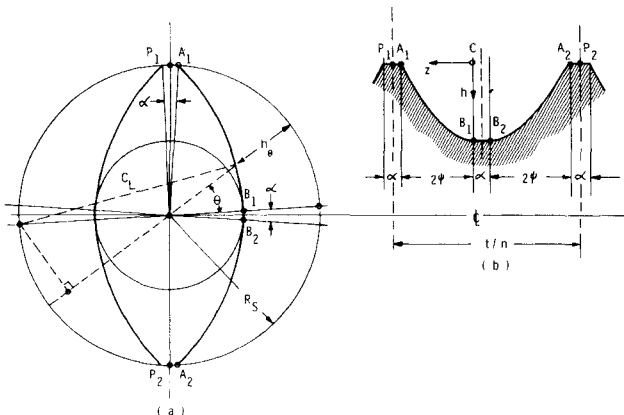


Fig. 16. Screw cross sections in plane through and perpendicular to the axis.

In this respect the development of Fig. 18b looks very much like the development of the single screw shown in Fig. 19, which has the same periphery, the same helix angle, and approximately the same channel cross section. The flow pattern in the nip zone OSTC of Fig. 18a does not contribute to the pressure generation, since the surface velocities of the screws oppose each other and the channel is symmetrical. Thus, a reasonable performance analysis has been obtained treating the twin screw as a single-screw pump with an equivalent diameter: $D_E = 2D(1 - \psi/\pi)$. The peripheral velocities must be the same in both cases. Note that the number of parallel channels in Fig. 18b is very nearly equal to $2n - 1$. The single-screw pump theory breaks down when the tip width is relatively large, such as in screw pumps with one tip.

The cross section of the channel is in part defined by Eq 9 adjusted for the helix angle. Shape factors for drag flow and pressure flow can be determined using the method previously developed for that purpose (4). Equations can be corrected for curvature (5) and end effects (6).

As in single-screw pumps, the average axial fluid velocity in partly full channels is approximately:

$$v_a = \frac{1}{2} N t \cos^2 \phi$$

Thus average retention times for flow through partly full

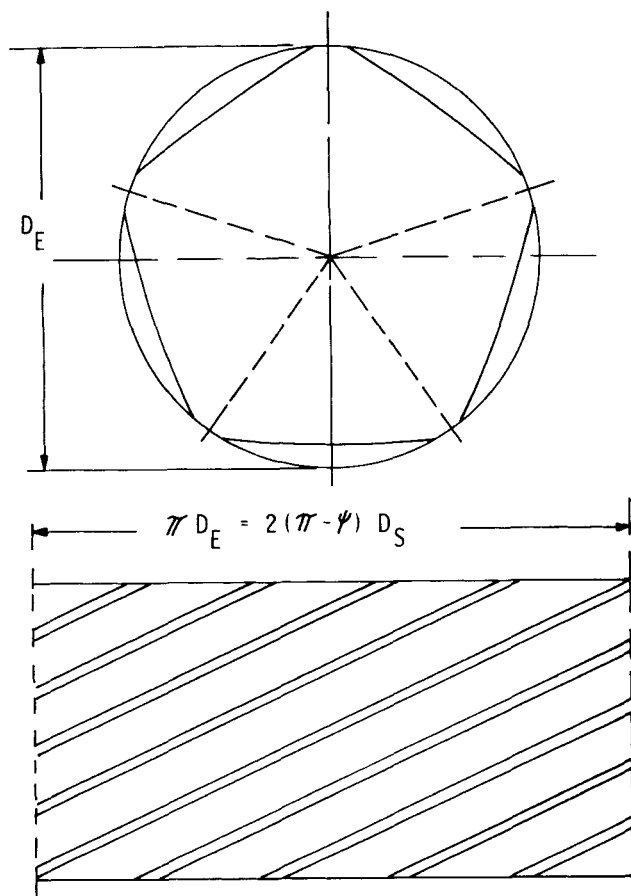


Fig. 19. Equivalent single screw and barrel development.

zones are inversely proportional to speed, independent of the free volume of the device.

SPECIFIC AREAS AND VOLUMES

For study of heat transfer, flow, and mass transfer in twin-screw equipment it is important to know the free volume between screws and barrel and the surface areas of screws and barrel. Data for specific volume and specific surface areas are presented here for geometrically similar screws, which are geometrically similar when they are fully wiped and have the same number of tips n , the same lead-to-diameter ratio t/D , and the same length-to-diameter ratio. Screw surface areas can be characterized by a geometric constant k , such that a typical area is given by:

$$A = k R_s^2 (L/D) \quad (10)$$

In a similar way, volumes of geometrically similar screws can be characterized by a geometric constant k_v , such that:

$$V = k_v R_s^3 (L/D) \quad (11)$$

Geometric constants will be derived for the barrel cross section, the screw or paddle cross section, the free cross section between barrel and screws, the screw and barrel surface area, and the free volume between barrel and screws. The barrel cross section is, from Fig. 15, equal to

$$A_{BC} = 2(\pi - \psi) R_s^2 + C_L R_s \sin \psi = k_{BC} R_s^2 \quad (12)$$

Thus, the barrel cross section coefficient k_{BC} is:

$$k_{BC} = 2(\pi - \psi) + \rho_c \sin \psi \quad (13)$$

This coefficient is a function of ρ_c only, since ψ can be expressed in ρ_c , Eq 1. Figure 20 shows k_{BC} as function of ρ_c . The cross-sectional area of a screw or paddle is, from Fig. 15, equal to:

$$A_D = n [\psi C_L^2 - C_L R_s \sin \psi] + \frac{1}{2} n \alpha (R_s^2 + R_B^2) = k_D R_s^2 \quad (14)$$

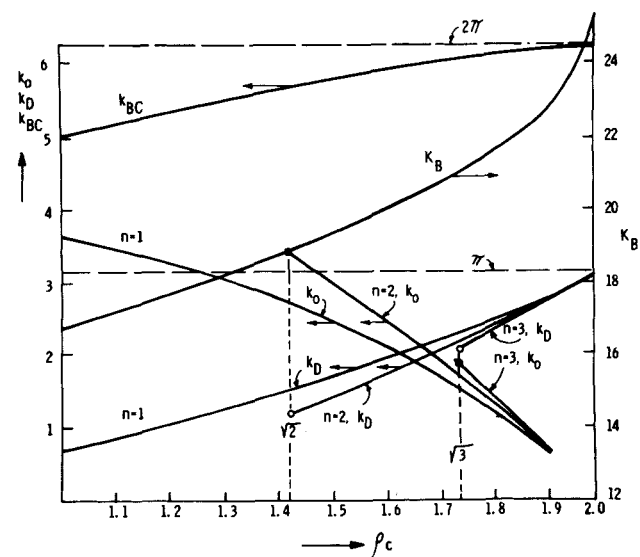


Fig. 20. Area and volume coefficients for corotating twin-screw equipment as function of the centerline ratio ρ_c with number of tips n as parameter.

The angle α is a function of n and ρ_c , Eq 5, while $R_B = C_L - R_S$. Thus

$$k_D = n[\psi\rho_c^2 - \rho_c \sin \psi + \frac{1}{2} \alpha(\rho_c - 1)^2] \quad (15)$$

The screw or disc cross section coefficient is a function of n and ρ_c . Figure 20 also shows that coefficient as a function of ρ_c with n as parameter. The free cross-sectional area between barrel and screws is:

$$A_o = A_{BC} - 2A_D = k_o R_s^2 \quad (16)$$

or:

$$k_o = k_{BC} - 2k_D \quad (17)$$

The free area coefficient k_o is also shown in Fig. 20. The free volume between barrel and screws is

$$V_o = A_o L = k_v R_s^3 (L/D) \quad (18)$$

Substitution of Eq 17 yields

$$k_v = 2k_o \quad (19)$$

The curves show that the maximum free volume is about the same for screw pumps with 1 or 2 tips and the same diameter and length, while the maximum volume for screws with three tips is smaller. These maxima are obtained at different centerline ratios ρ_c . The curves for k_D are useful for estimation of weight or displacement of screws and paddles.

The outside surface A_p of a straight paddle or disc is the product of its periphery and length L . That periphery is:

$$p = n[\alpha(R_s + R_B) + 2C_L^\psi] \quad (20)$$

Substitution of Eq 4 yields the interesting result:

$$p = \pi C_L = \pi \rho_c R_s \quad (21)$$

The paddle surface area and area coefficient become:

$$A_p = \pi \rho_c R_s L, \quad k_p = 2\pi \rho_c \quad (22)$$

This surface area includes the surface of the tips.

The surface area of a screw consists of three types of surface: one generated by the tip, the second generated by the root, and the third generated by the flanks. The surface area generated by one tip is:

$$A_T = \alpha R_s L = 2 \alpha R_s^2 (L/D) \quad (23)$$

Similarly, one root curve generates an area:

$$A_R = \alpha R_B L = 2 \alpha R_s^2 (\rho_c - 1)(L/D) \quad (24)$$

The surface area A_{C1} generated by one flank can be expressed as:

$$A_{C1} = k_{C1} R_s^2 (L/D) \quad (25)$$

The calculation of k_{C1} is shown in Appendix B. The total surface area of one screw becomes:

$$A_{S1} = n[A_T + A_R + 2A_{C1}] = k_{S1} R_s^2 (L/D) \quad (26)$$

The screw surface area coefficient k_{S1} is shown in Figs. 21-23 as a function of the lead-to-diameter ratio with ρ_c

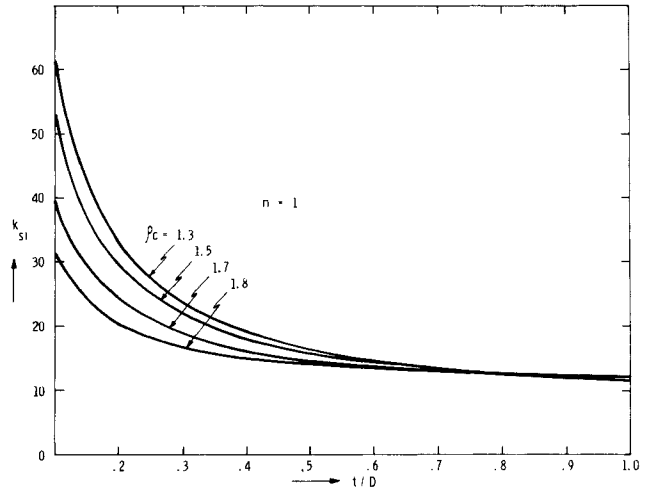


Fig. 21. Screw surface area coefficient k_{S1} as function of lead-to-diameter ratio for screws with one tip.

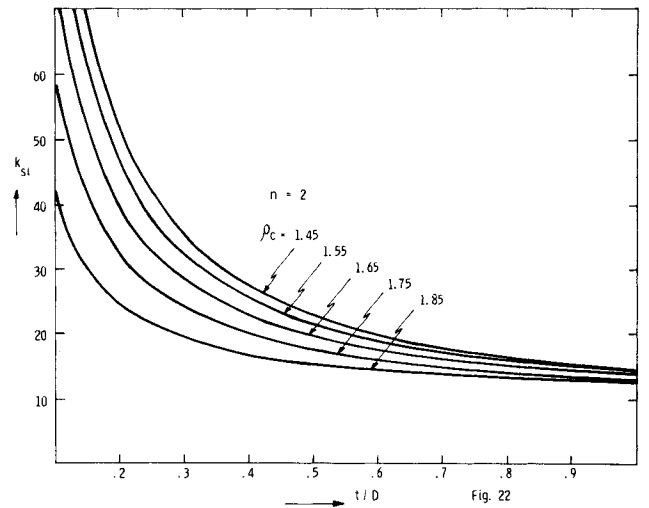


Fig. 22. Screw surface area coefficient k_{S1} as function of lead-to-diameter ratio for screws with two tips.

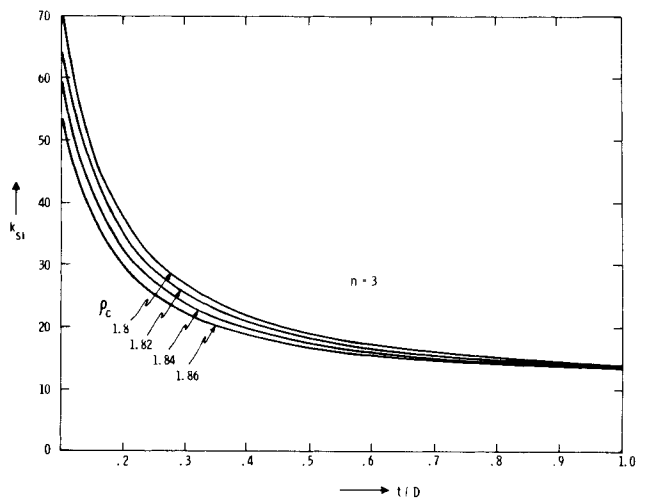


Fig. 23. Screw surface area coefficient k_{S1} as function of lead-to-diameter ratio for screws with three tips.

as parameter for screws with 1, 2, and 3 tips. Note that this coefficient also includes the area of the tips. The limit for k_{S1} for infinite leads is, from Eq 22, equal to

$$k_{S1L} = 2\pi\rho_c \quad (28)$$

For small t/D ratios, k_{S1} is very nearly hyperbolic in t/D .

The effective volume coefficients for screws with clearances will be larger than k_v . For a given clearance between the tip of one screw and the surface of its mate, the volume increases by the product of surface area and clearance, so effective coefficients can be calculated using both k_v and k_{S1} .

The surface area of a twin-screw barrel is the product of its periphery and length. The periphery is:

$$p = 2D(\pi - \psi) \quad (29)$$

The barrel surface is:

$$A_B = 2LD(\pi - \psi) = k_B R_s^2 (L/D) \quad (30)$$

The dimensionless barrel area coefficient becomes:

$$k_B = \delta[\pi - \cos^{-1}(\rho_c/2)] \quad (31)$$

This coefficient is also shown in Fig. 20.

SUMMARY

In this paper we deal with the geometry of corotating fully wiped twin screws such as those used in extruders, evaporators, and other types of processing equipment. The geometry of cross sections for such screws is derived using a well-known kinematic principle: One screw cross section is brought to a standstill, and the cross section of its mate is made to execute the proper relative motion. Resulting screw cross sections are unique for a given screw diameter, centerline distance, and number of tips. In graphical form we present the unique relationship between tip angle, number of tips, and ratio of centerline to screw radius for conventional pairs of screws with the same diameter, operating at the same speed. Similar results are shown for the less common screws with different diameters and/or a speed ratio. The relative motion is depicted for a number of examples, both for conventional and unconventional screws.

It is shown that, although there is a seal between adjacent screw channels, there is an open passage from one screw to its mate. For screws with reasonably small tip angles there are continuous channels in the equipment, giving open communication between inlet and discharge. Flow in the nip between screws does not contribute significantly to fluid transport. Thus it is possible to make a reasonable flow analysis by substituting a single-screw device with the same barrel periphery, the same helix angle, $2n-1$ channels, and a similar channel depth distribution. A different analysis applies to partly full channels where average velocities are proportional to speed and retention times are inversely proportional to speed, independent of flow rate or free volume.

For study of flow, and heat and mass transfer, one must know screw surface areas and free volumes between screws and barrel. Geometrically similar screws

have surface areas proportional to D^2 and volumes proportional to D^3 . Proportionality coefficients are given for screws as functions of the centerline distance ratio, number of screw tips, and lead-to-diameter ratios.

APPENDIX A

The construction of cross sections for corotating screws with a diameter and/or speed difference is somewhat more complicated than for identical screws, since flank curves are no longer circular. We start with disc A having a radius R_1 and rotational speed ω_1 , disc B with radius R_2 and speed ω_2 , with centerline distance C_L .

In this system there are two centerline ratios and a speed ratio m . It is simpler to use inverse centerline ratios:

$$k_1 = R_1/C_L, \quad k_2 = R_2/C_L \quad (A-1)$$

We determine first how cross sections of screws must be constructed. Next we must determine allowable combinations of m , k_1 , and k_2 , that will result in positive tip angles. First we discuss the construction of flank curves.

Figure A-1 shows the construction of the trajectory described on disc A by a point P on disc B. Now we add a motion $-\omega_1$ around O to the whole system to bring disc A to a standstill. The trajectory of C is again a circle with radius C_L and center at O. Disc B still rotates with a relative velocity $\omega_2 - \omega_1$ which is counter clockwise when $\omega_1 > \omega_2$ as assumed in Fig. A-1. OC_1 rotates with $-\omega_1$, C_1P_1 with $\omega_2 - \omega_1$. Assume that disc A has n_1 tips, disc B n_2 tips, and let m be the speed ratio, then:

$$m = \omega_2/\omega_1 = n_1/n_2 \quad (A-2)$$

Angle γ_1 is related to angle θ_1 by:

$$\gamma_1/\theta = \frac{\omega_1 - \omega_2}{\omega_1} = 1 - m \quad (A-3)$$

The coordinates of the trajectory for P, expressed in terms of the rotation angle θ , become:

$$x_p = C_L \cos \theta - R_2 \cos [(1 - m) \theta] \quad (A-4)$$

$$y_p = C_L \sin \theta - R_2 \sin [(1 - m) \theta] \quad (A-5)$$

The trajectory in polar coordinates and in the centerline ratios becomes:

$$r_p = C_L [1 + k_2^2 - 2k_2 \cos (m \theta)]^{1/2} \quad (A-6)$$

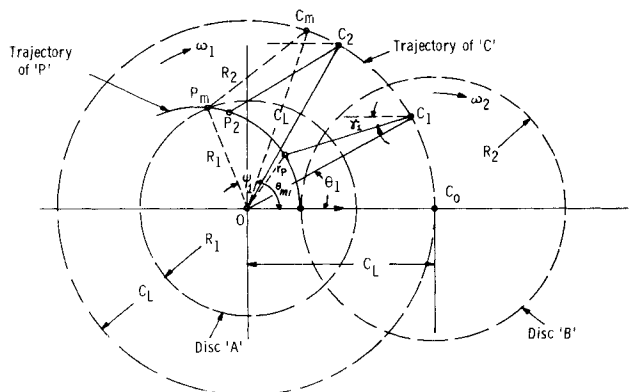


Fig. A-1. Construction of trajectory for P for screws with different diameters and different speeds.

This then is the flank curve. To determine the tip angle we must know angle ϕ_{m1} where the trajectory intersects the tip circle $r = R_1$. This occurs at $\theta = \theta_{M1}$, or when

$$k_1^2 = 1 + k_2^2 - 2k_2 \cos(m \theta_{M1}) \quad (\text{A-7})$$

Thus

$$\theta_{M1} = \frac{1}{m} \cos^{-1} \left[\frac{1 + k_2^2 - k_1^2}{2k_2} \right] \quad (\text{A-8})$$

Next we must determine angle ψ_1 . Three sides R_1 , R_2 and C_L are known in triangle $OP_m C_m$, so:

$$\cos \psi_1 = \frac{C_L^2 + R_1^2 - R_2^2}{2C_L R_1} \quad (\text{A-9})$$

or, in terms of centerline ratios:

$$\cos \psi_1 = \frac{1 + k_1^2 - k_2^2}{2k_1} \quad (\text{A-10})$$

The polar angle ϕ_{m1} of P_m then becomes:

$$\phi_{m1} = \cos^{-1} \left(\frac{1 + k_1^2 - k_2^2}{2k_1} \right) + \frac{1}{m} \cos^{-1} \left(\frac{1 + k_2^2 - k_1^2}{2k_2} \right) \quad (\text{A-11})$$

The 'flank' curve or trajectory is fully defined by Eqs A-10 and A-11. Next we must define the 'root' curve.

Figure A-2 shows the motion of the circular tip of disc B relative to disc A during the wiping of the circular root curve of disc A. The two extreme positions are shown for a tip bounded by an arc $P_o Q_o$ for a tip angle α_2 on disc B. In the first position Q_o lies on the line connecting C_o and O , in the second one P_m lies on the line connecting O with the present center C_m of disc B. Q_o is the start (or end) of the trajectory or the flank curve of Q , P_m the start of the trajectory for P . The line $C_n Q_n$ is not horizontal for this case, but makes an angle $(1 - m) \beta_1$ with the horizontal. From Fig. A-2:

$$\alpha_2 = \beta_1 - (1 - m) \beta_2 \quad (\text{A-12})$$

or

$$\alpha_2 = m \beta_1 \quad (\text{A-13})$$

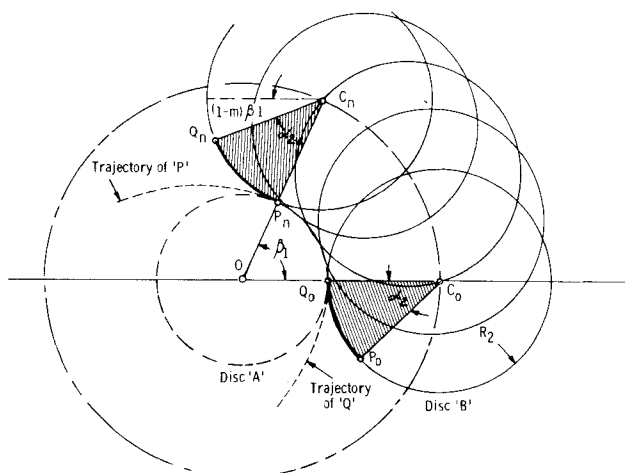


Fig. A-2. Envelope of positions occupied by tip PQ during relative motion of screws with a speed ratio $m \neq 1.0$.

By a similar argument we can prove that the tip angle α_1 of disc A is related to the root angle β_2 of disc B by:

$$\alpha_1 = \beta_2/m \quad (\text{A-14})$$

We are free to select the ratio α_1/β_1 . From Eqs 19 and 20:

$$\frac{\alpha_2}{\beta_2} = \frac{\beta_1}{\alpha_1} \quad (\text{A-15})$$

Thus, the ratio of the root-to-tip angles of one disc is the inverse of that of its mate, except that it is equal to 1 for the case $\alpha_1 = \beta_1$.

A disc with n_1 tips has $2n_1$ flank angles ϕ_{m1} , n_1 tip angles and n_1 root angles. For the case that $\alpha_1 = \beta_1$:

$$2n_1(\alpha_1 + \phi_{m1}) = 2\pi \quad (\text{A-16})$$

or

$$\alpha_1 = \pi/n_1 - \cos^{-1} \left(\frac{1 + k_1^2 - k_2^2}{2k_1} \right) - \frac{1}{m} \cos^{-1} \left(\frac{1 + k_2^2 - k_1^2}{2k_2} \right) \quad (\text{A-17})$$

Tip angle α_1 must be positive, so m must be larger than:

$$m \geq \frac{\cos^{-1} [(1 + k_1^2 - k_2^2)/2k_1]}{\pi/n_1 - \cos^{-1} [(1 + k_1^2 - k_2^2)/2k_1]} = m_{min} \quad (\text{A-18})$$

The minimum value for m is shown for $n_1 = 1$ in Fig. 9 as function of k_1 with k_2 as parameter. For instance, for $k_1 = 0.625$, $k_2 = 0.90$ the minimum ratio is $m_{min} = 0.3225$, so a speed ratio $m = 0.333$, or $n_2 = 3$, is allowed. Additional restrictions are:

$$\begin{aligned} (R_1 + R_2) &> C_L \text{ or: } k_1 + k_2 > 1.0 \\ R_1 &< C_L \text{ or: } k_1 < 1.0 \\ R_2 &< C_L \text{ or: } k_2 < 1.0 \end{aligned} \quad (\text{A-19})$$

Curve sheets similar to Fig. 9 can be constructed for different values of n_1 . For the simpler case of equal diameter with a speed ratio m :

$$k_1 = k_2 = 1/\rho_c \quad (\text{A-20})$$

For that case Eq A-17 reduces to:

$$\alpha_1 = \pi/n_1 - (1 + \frac{1}{m}) \cos^{-1}(\rho_c/2) \quad (\text{A-21})$$

or

$$\rho_c = 2 \cos \left[\frac{m}{1 + m} (\pi/n_1 - 1) \right] \quad (\text{A-22})$$

Figure 10 shows the relation between ρ_c and α_1 with n_1 and m as parameters. The curves for $m = 1$ are of course identical to those of Fig. 4.

APPENDIX B

To derive an equation for the surface area generated by the flank curve consider the screw surface geometry in the proximity of a point P of the cross section shown in Fig. B-1. Q is a neighboring point on the flank curve, so PQ lies on the screw surface. S lies on QO such that $SO = SP = r$. In an elementary analysis S and P lie on a cylinder with radius r , so the area of a helical strip

through SP has an area:

$$dA_1 = Lr \, d\theta \quad (B-1)$$

Through S we can draw a line parallel to the screw axis. That line is perpendicular to the plane of the screw cross section and perpendicular to SP . We can also draw the helical curve through P . These two lines intersect at T when we make $d\theta$ small enough. The triangle QTP is now an element of the screw surface, while triangle STP is part of dA_1 . Figure B-1 (b) shows the angle γ between the lines SG and QG , which are in a plane normal to PT . Note that ΔSPT is equal to the local helix angle ϕ_r , which is:

$$\phi_r = \tan^{-1}(t/2\pi r) \quad (B-2)$$

Now:

$$\cos \gamma = SG/QG = \sin \phi_r / \sqrt{\sin^2 \phi_r + \tan^2 \beta} \quad (B-3)$$

Also:

$$\angle MPO = \beta$$

so:

$$\tan \beta = \frac{R_s \sin \theta}{\sqrt{C_L^2 - R_s^2 \sin^2 \theta}} = \frac{\sin \theta}{\sqrt{\rho_c^2 - \sin^2 \theta}} \quad (B-4)$$

Substitution in Eq B-3 yields:

$$\cos \gamma = \frac{\sin \phi_r}{\sqrt{\sin^2 \phi_r + \sin^2 \theta / (\rho_c^2 - \sin^2 \theta)}} \quad (B-5)$$

Radius r can be expressed in θ and the known dimensions C_L and R_s , since PF can be written as:

$$r + R_s \cos \theta = \sqrt{C_L^2 - R_s^2 \sin^2 \theta} \quad (B-6)$$

The surface generated by one flank curve becomes:

$$A_{C1} = \int_0^{2\psi} \left(\frac{Lr}{\sin \phi_r} \right) \sqrt{\sin^2 \phi_r + \frac{\sin^2 \theta}{\rho_c^2 - \sin^2 \theta}} \, d\theta$$

$$= k_{C1} R_s^2 (L/D) \quad (B-7)$$

Substitution of Eq B-6 yields after some algebra:

$$k_{C1} = 2 \int_0^{2\psi} \left\{ \sqrt{\rho_c^2 - \sin^2 \theta} - \cos \theta \right\} \sqrt{1 + \frac{\sin^2 \theta}{\sin^2 \phi_r (\rho_c^2 - \sin^2 \theta)}} \, d\theta \quad (B-8)$$

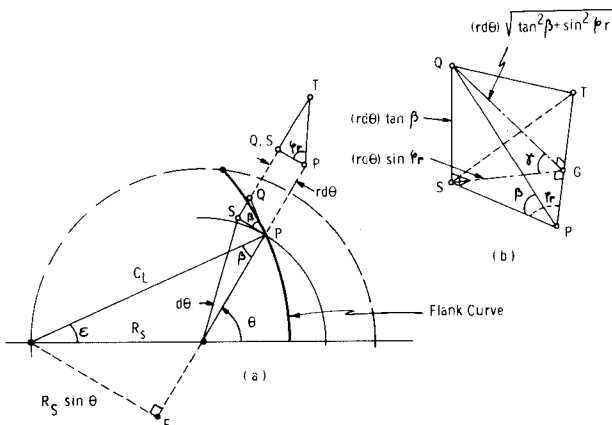


Fig. B-1. Screw surface area element.

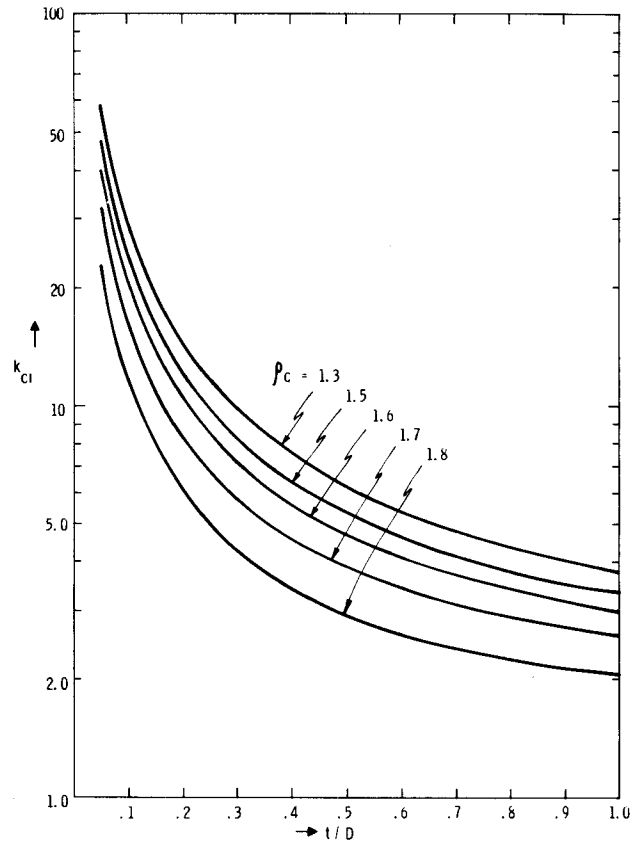


Fig. B-2. Area coefficient k_{C1} for surface described by one flank curve, as function of t/D with ρ_c as parameter.

This integration was carried out numerically. It should be noted that k_{C1} is independent of the number of tips n and a function only of ρ_c and t/D . Figure B-2 shows k_{C1} as function of t/D with ρ_c as the parameter.

NOMENCLATURE

A	= area
A_B	= barrel surface area
A_D	= disc area
A_o	= free cross sectional area between screws and barrel, normal to axis
A_p	= paddle surface area
A_T	= tip surface area
A_R	= surface area of root
A_{C1}	= surface area generated by one flank curve
A_{S1}	= combined surface area of one screw
C_L	= centerline distance between screws or discs
D	= screw diameter
h	= channel depth
k_1, k_2	= inverse centerline ratio
k_B	= barrel surface area coefficient
k_D	= disc area coefficient
k_S	= free volume coefficient
k_o	= free cross sectional coefficient
k_p	= paddle surface area coefficient
k_{C1}	= area coefficient for one flank curve
k_{S1}	= screw surface area coefficient
L	= length of screw, axial
N	= rotational speed, revolutions per unit time
n, n_1, n_2	= number of tips

p	= periphery of cross section
R_1, R_2	= screw radii
R_s	= screw or disc outside radius
t	= lead of screw
V	= volume
v	= velocity
x_p, y_p	= coordinates of flank curves
z	= axial coordinate
α	= tip angle in plane perpendicular to axis
β	= root angle in plane perpendicular to axis
ρ	= centerline distance C_L/R_s
ψ	= angle defined in Eq 1

κ	= relative channel depth
θ	= coordinate
ϕ	= helix angle
ω	= rotational speed

REFERENCES

1. R. Erdmenger, U.S. Pat. 2,670,188, Feb. 23, 1954.
2. H. G. Zimmerman, U.S. Pat. 3,170,566, Feb. 23, 1965.
3. B. M. Pinney, U.S. Pat. 3,717,330, Feb. 20, 1973.
4. M. L. Booy, *Trans. ASME, Series D*, **88**, 725 (1966).
5. M. L. Booy, *Trans. ASME, Series B*, **86**, 22 (1964); *Trans. SPE* **3**, 176 (1963); *Kautchuk und Gummi-Kunststoffe*, **17**, p. 26' (1964).
6. M. L. Booy, *Trans. ASME, Series D*, **88**, 121 (1966).